Absorptive nature of scattering coefficients in stress-energy tensor formalism for room acoustics

Jean-Dominique Polack, Hugo Dujourdy, Roland Badeau

Absorptive nature of scattering coefficients in stress-energy tensor formalism for room acoustics

Jean-Dominique Polack,[1,2,3] Hugo Dujourdy,[1,2,3] and Roland Badeau[1,2,3]

[1)] *Sorbonne Université, CNRS UMR 7190, Institut Jean le Rond d'Alembert, F-75005 Paris, France*

[2] *Diffusion Acoustic, F-92150 Suresnes, France*

[3] *LTCI, Télécom Paris, F-91120 Palaiseau, France*[a]

(Dated: 21 February 2024)

In the stress-energy tensor formalism, the symmetry between absorption and scattering coefficients, as proven by measurements combined with simulations, is counter-intuitive. By introducing the wall admittance, we show that the scattering coefficient is partly created by the real part of the wall admittance combined with the active intensity, that is, is partly due to absorption. However, for curved surfaces or finite source distances, it also depends on the imaginary part of the wall admittance in combination with the reactive intensity, which confers it genuine scattering properties inversely proportional to the distances to the sources. Thus, for plane waves impinging on plane boundaries, or purely real admittances, scattering reduces to absorption.

[a)] jean-dominique.polack@sorbonne-universite.fr

I. INTRODUCTION

(Added: The stress-energy tensor formalism was initially introduced by Morse and collaborators (Morse and Feshbach, 1956; Morse and Ingard, 1968) in order to describe energy conservation in linear acoustics. Many years later, Stanzial and collaborators applied the conservation of the stress-energy tensor to room acoustics (Stanzial *et al.*, 2002), focusing on the expression of the radiation pressure. In a subsequent paper (Stanzial and Schiffrer, 2010), they introduced the energy velocity as ratio of the sound intensity to the total acoustic energy, and derived from the conservation of the stress-energy tensor an expression for the local inital reverberation time at the onset of energy decay. Some related ideas, linking wave impedance to the complex sound intensity, are also found in (Mann *et al.*, 1987; Stanzial and Graffigna, 2017). Mann *et al.* focused on energy transfer and analysed in terms of energy flux and power what happens in the vicinity of intensity vortex that are created by specific configurations of sources. Stanzial and Graffigna went one step further in the definition and measurement of complex intensity. However, both papers are outside the scope of the present analysis that focuses on the active stress-energy tensor - see (Polack, 2023) for an extension to the *complex* stress-energy tensor and its conservation, together with preliminary measurement results.)

(Replaced: ~~The stress-energy tensor formalism~~ replaced with: A somewhat different perspective) was introduced by Dujourdy *et al.* (Dujourdy *et al.*, 2017, 2019) (Added: in order) to generalize the diffusion equation formalism of Ollendorff and Picaut (Ollendorff, 1969; Picaut *et al.*, 1997). Indeed, where the diffusion equation arbitrarily introduces a gradi-

ent type relationship between sound intensity and total energy, the stress-energy tensor formalism introduces instead the conservation equation for intensity. When integrated in disproportionate enclosures, the stress-energy tensor yields both absorption and scattering on the boundaries. Dujourdy *et al.* stressed the symmetrical role played by absorption and scattering coefficients in the conservation equations, which was then systematically investigated and confirmed by Meacham *et al.* (Meacham *et al.*, 2019). The present papers aims at proving this symmetry and the absorbing nature of the scattering coefficient, using the local admittance formalism at the boundaries.

After presenting the background of the stress-energy conservation, we successively express the elements of the stress energy tensor on the boundaries, then the absorption and scattering coefficients, in terms of the local admittance. We then examine the main types of boundaries, and discuss the relationship between absorption and scattering coefficients.

II. THE BASIC EQUATIONS

Dujourdy *et al.* (Dujourdy *et al.*, 2017, 2019) have shown that the wave equation, satisfied by the velocity potential, can be extended by a set of conservation equations that reduces to the conservation of the stress-energy tensor $\underline{\underline{T}}$.

Let ψ be the velocity potential. The conservation of the stress-energy tensor is expressed as:

$$\vec{\nabla} \cdot \underline{\underline{T}} = 0 \tag{1}$$

with

$$\underline{\underline{T}} = \begin{pmatrix} E_{tt} & E_{tx} & E_{ty} & E_{tz} \\ E_{tx} & E_{xx} & E_{xy} & E_{xz} \\ E_{ty} & E_{xy} & E_{yy} & E_{yz} \\ E_{tz} & E_{xz} & E_{yz} & E_{zz} \end{pmatrix}$$

In terms of the velocity potential, the elements of the stress-energy tensor are given by:

$$\begin{aligned}
E_{tt} &= \tfrac{\rho}{2}(\tfrac{1}{c^2}|\partial_t\psi|^2 + |\vec{\nabla}\psi|^2) \\
E_{tx} &= -\tfrac{\rho_0}{c}\partial_t\psi\partial_x\psi \\
E_{ty} &= -\tfrac{\rho_0}{c}\partial_t\psi\partial_y\psi \\
E_{tz} &= -\tfrac{\rho_0}{c}\partial_t\psi\partial_z\psi \\
E_{xx} &= \tfrac{\rho_0}{2}(\tfrac{1}{c^2}|\partial_t\psi|^2 + |\partial_x\psi|^2 - |\partial_y\psi|^2 - |\partial_z\psi|^2) \\
E_{yy} &= \tfrac{\rho_0}{2}(\tfrac{1}{c^2}|\partial_t\psi|^2 - |\partial_x\psi|^2 + |\partial_y\psi|^2 - |\partial_z\psi|^2) \\
E_{zz} &= \tfrac{\rho_0}{2}(\tfrac{1}{c^2}|\partial_t\psi|^2 - |\partial_x\psi|^2 - |\partial_y\psi|^2 + |\partial_z\psi|^2) \\
E_{xy} &= \rho_0\partial_x\psi\partial_y\psi \\
E_{xz} &= \rho_0\partial_x\psi\partial_z\psi \\
E_{yz} &= \rho_0\partial_y\psi\partial_z\psi
\end{aligned}$$

where ρ_0 is the (Added: steady-state) density of air and c the speed of sound.

In the specific cases of long enclosures (Dujourdy *et al.*, 2017) and flat spaces (Dujourdy *et al.*, 2019), Dujourdy *et al.* were able to reduce the conservation of the stress-energy tensor

(eq. 1) to the telegraphers equation:

$$\frac{1}{c^2}\partial_{tt}E - \partial_{xx}E + \frac{A+D}{\lambda c}\partial_t E + \frac{AD}{\lambda^2}E = 0 \tag{2}$$

where E is the total energy, λ is the mean free path of the enclosure, and A and D are respectively modified absorption and scattering coefficients at the boundaries. Eq. (2) is symmetrical with respect to the absorption and scattering coefficients, as was confirmed by Meacham *et al.* (Meacham *et al.*, 2019) who systematically explored the whole space of values for the absorption and scattering coefficients and compared thus obtained reverberation times and spatial decays with the measured ones in a hallway. As shown in Fig. 1, the measured reverberation times and spatial decays correspond to narrow stripes of values for A and D, which do not always overlap; but most striking in Fig. 1 is the symmetry of the figure with respect to absorption and scattering coefficients. Physical justification of this symmetry is therefore the goal of the present paper.

III. WALL ADMITTANCE

Now, wall admittance introduces a relation between the normal derivative and the time derivative of the velocity potential on the wall:

$$-\partial_n\psi = \frac{\beta}{c}\partial_t\psi = \frac{1}{c\zeta}\partial_t\psi$$

with $\vec{n}$ the exterior normal to the wall, ζ the (Replaced: ~~reduced~~ replaced with: specific acoustic) impedance of the wall (Added: (Morse and Ingard, 1968, p. 580)), (Added: that is, the wall impedance normalized by the characteristic impedance $\rho_0 c$ of air,) and $\beta = \frac{1}{\zeta}$

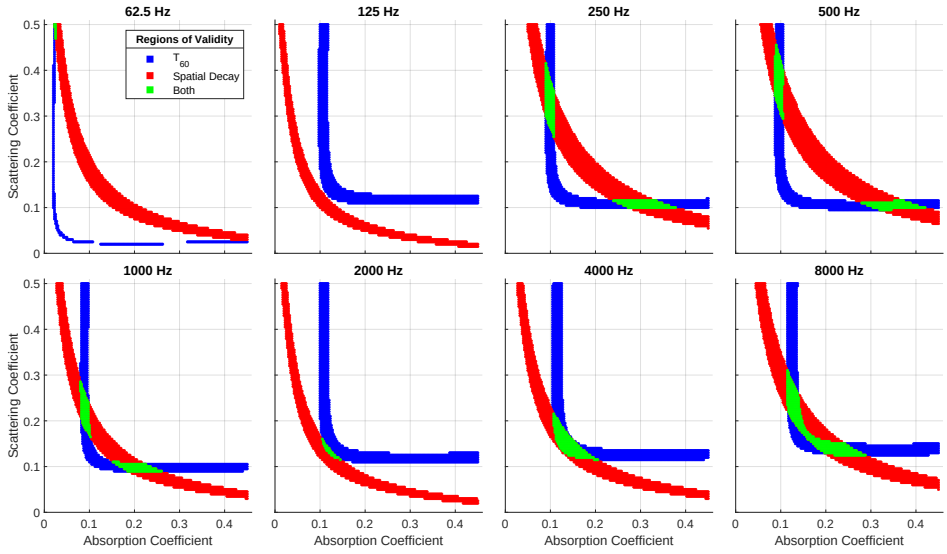

FIG. 1. Relevant combinations of absorption and scattering coefficients leading to measured reverberation times and spatial decays in a hallway (reproduced from (Meacham *et al.*, 2019)).

(Added: is) the (Replaced: ~~reduced~~ replaced with: specific acoustic) admittance. Let us then consider a flat enclosure with vertical coordinate z. We can express the elements $E_{\cdot z}$ of the stress-energy tensor, where $\cdot$ takes the values t, x, or y. However, the admittance formalism implies a complex velocity potential, whereas the elements of the stress-energy tensor must remain real, as is expected from energy quantities. Thus, the expression for the

non-diagonal terms of the stress-energy tensor must be modified as:

$$
\begin{aligned}
E_{tx} &= -\tfrac{\rho_0}{c}\,\Re(\partial_t\psi\partial_x\psi^*) \\
E_{ty} &= -\tfrac{\rho_0}{c}\,\Re(\partial_t\psi\partial_y\psi^*) \\
E_{tz} &= -\tfrac{\rho_0}{c}\,\Re(\partial_t\psi\partial_z\psi^*) \\
E_{xy} &= \rho_0\,\Re(\partial_x\psi\partial_y\psi^*) \\
E_{xz} &= \rho_0\,\Re(\partial_x\psi\partial_z\psi^*) \\
E_{yz} &= \rho_0\,\Re(\partial_y\psi\partial_z\psi^*)
\end{aligned}
$$

where the exponent $*$ means complex conjugated.

We thus obtain on the "ceiling":

$$
\begin{aligned}
E_{tz} &= \tfrac{\rho_0}{c^2}\,\Re(\partial_t\psi\beta^*\partial_t\psi^*) = \tfrac{\rho_0}{c^2}\Re(\beta)|\partial_t\psi|^2 \\
E_{xz} &= -\tfrac{\rho_0}{c}\,\Re(\partial_x\psi\beta^*\partial_t\psi^*) = \Re(\beta)\,E_{tx} + \Im(\beta)\,\Im(\tfrac{\rho_0}{c}\partial_x\psi\partial_t\psi^*) \\
E_{yz} &= -\tfrac{\rho_0}{c}\,\Re(\partial_y\psi\beta^*\partial_t\psi^*) = \Re(\beta)\,E_{ty} + \Im(\beta)\,\Im(\tfrac{\rho_0}{c}\partial_y\psi\partial_t\psi^*)
\end{aligned}
\tag{3}
$$

and the same equations with opposite sign on the "floor". (Added: Note that E_{xz} and E_{yz} correspond to the parallel components of the radiation pressure exerted on the "ceiling" and the "floor" (Stanzial *et al.*, 2002).)

IV. INTERPRETATION

Recalling that E_{tx} and E_{ty} are the components of the sound intensity in the x and y directions, we observe that the boundary conditions for E_{xz} and E_{yz} involve not only the active intensity associated with the real part of the admittance, but also the reactive

intensity associated with the imaginary part of the admittance. This is not surprising, as the reactive intensity corresponds to local recirculation of energy, just as the imaginary part of the wall admittance is associated with a non-flat surface. Both phenomena contribute to the scattering of the impinging waves.

However, recalling that admittances are defined for pure waves only, we can further simplify these expressions by considering the phase angles ϕ_x and ϕ_y between the space derivatives of the velocity potential with respect to x and y respectively, and its time derivative. The last two ceiling equations then reduce to:

$$E_{xz} = [\Re(\beta) + \Im(\beta)\, \tan\phi_x]\, E_{tx}$$

$$E_{yz} = [\Re(\beta) + \Im(\beta)\, \tan\phi_y]\, E_{ty}$$

As for E_{tz}, we must first express E_{tt} as a function of the wall admittance, that is:

$$\begin{aligned} E_{tt} &= \tfrac{\rho_0}{2}(\tfrac{1}{c^2}|\partial_t\psi|^2 + |\vec{\nabla}\psi|^2) \\ &= \tfrac{\rho_0}{2}(\tfrac{1}{c^2}|\partial_t\psi|^2 + |\partial_x\psi|^2 + |\partial_y\psi|^2 + |\partial_z\psi|^2) \\ &= \tfrac{\rho_0}{2}(\tfrac{1}{c^2}|\partial_t\psi|^2 + |\partial_x\psi|^2 + |\partial_y\psi|^2 + |\tfrac{\beta}{c}\partial_t\psi|^2) \\ &= \tfrac{\rho_0}{2}(\tfrac{1}{c^2}[1 + |\beta|^2]\,|\partial_t\psi|^2 + |\partial_x\psi|^2 + |\partial_y\psi|^2) \end{aligned}$$

Introducing the angle of incidence θ of the wave makes it possible to express the last two terms in the previous equation as:

$$|\partial_x\psi|^2 + |\partial_y\psi|^2 = \frac{\sin^2\theta}{c^2}|\partial_t\psi|^2$$

that is:

$$E_{tt} = \frac{\rho_0}{2c^2}(1 + \sin^2\theta + |\beta|^2)\,|\partial_t\psi|^2 \tag{4}$$

leading to the following expression for the absorption coefficient:

$$\alpha(\theta) = \frac{E_{tz}}{E_{tt}} = \frac{2\,\Re(\beta)}{1 + \sin^2\theta + |\beta|^2} \tag{5}$$

The interpretations of the scattering coefficients D_x and D_y are similar. We simply obtain:

$$\begin{aligned} D_x &= \tfrac{E_{xz}}{E_{tx}} = [\Re(\beta) + \Im(\beta)\,\tan\phi_x] \\ D_y &= \tfrac{E_{yz}}{E_{ty}} = [\Re(\beta) + \Im(\beta)\,\tan\phi_y] \end{aligned} \tag{6}$$

V. BOUNDARY CONDITIONS

The evaluation of eqs. (6) takes different forms depending on the type of boundary and the position of the source.

A. Plane wave on flat boundary

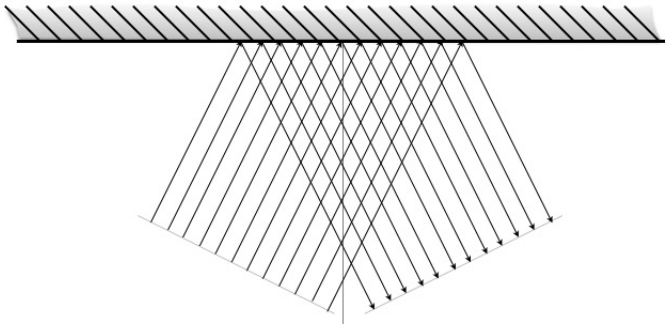

FIG. 2. Plane wave reflecting on flat boundary.

For a plane wave impinging on a flat boundary $z = 0$ (Fig. 2), the velocity potential takes the following form:

$$\psi(t, r) = \exp -i(\omega t - k_x x - k_y y - k_z z) + R \exp -i(\omega t - k_x x - k_y y + k_z z) \tag{7}$$

where ω is the radian frequency, k_x, k_y and k_z the components of the wave number $k = \frac{\omega}{c}$ along the three coordinates, and R the complex reflection coefficient on the boundary. The first term in eq. (7) represents the impinging wave; and the second the reflected wave. The time derivative in the neighbourhood of the boundary is given by:

$$\partial_t \psi = -i\omega\psi = -i\omega \exp -i(\omega t - k_x x - k_y y) \left[\exp ik_z z + R \exp -ik_z z\right]$$

and the space derivatives by:

$$\begin{aligned}
\partial_x \psi &= ik_x\psi = ik_x \exp -i(\omega t - k_x x - k_y y) \left[\exp ik_z z + R \exp -ik_z z\right] = -\tfrac{k_x}{\omega}\partial_t\psi \\
\partial_y \psi &= ik_y\psi = ik_y \exp -i(\omega t - k_x x - k_y y) \left[\exp ik_z z + R \exp -ik_z z\right] = -\tfrac{k_y}{\omega}\partial_t\psi \\
\partial_z \psi &= ik_z \exp -i(\omega t - k_x x - k_y y) \left[\exp ik_z z - R \exp -ik_z z\right] = -\tfrac{\beta}{c}\partial_t\psi
\end{aligned} \tag{8}$$

As a consequence, on the boundary $z = 0$, the phase angles ϕ_x and ϕ_y between the space derivatives of the velocity potential with respect to x and y and its time derivative are both equal to 0. In this case, eqs. (6) simply reduce to:

$$D_x = D_y = \Re(\beta)$$

that is, the scattering coefficient is purely created by absorption. Note that the last line of eq. (8), together with the relation between the normal component of the wave number and the angle of incidence $k_z = k\cos\theta = \frac{\omega}{c}\cos\theta$, gives the expected relation between the complex reflection coefficient and the admittance:

$$R = \frac{\cos\theta - \beta}{\cos\theta + \beta} = \frac{[\cos^2\theta - |\beta|^2] - 2i\cos\theta\Im\beta}{\cos^2\theta + 2\cos\theta\Re\beta + |\beta|^2}$$

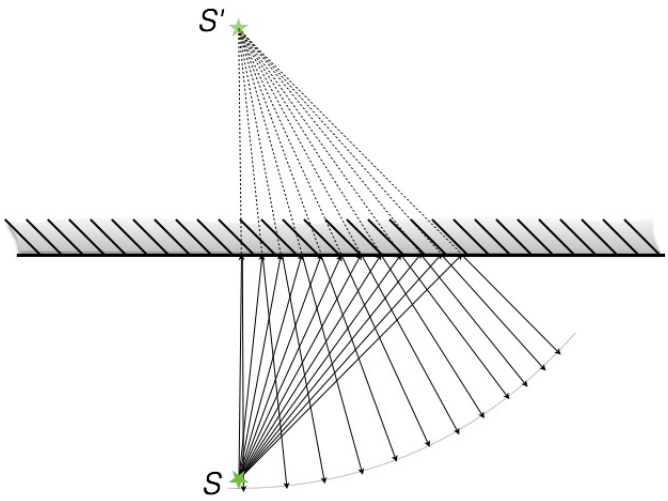

FIG. 3. Source at finite distance from flat boundary; S is real source, and S' virtual image source.

B. Source at finite distance from flat boundary

For a spherical wave impinging on a flat boundary (Fig. 3), the velocity potential takes a different form:

$$\psi(t,r) = \frac{\exp -i(\omega t - kr)}{4\pi r} + R\frac{\exp -i(\omega t - kr')}{4\pi r'} \tag{9}$$

where R still is the complex reflection coefficient on the boundary, r the distance to the real source S, and r' the distance to the virtual image source S' (see Fig. 3). The first term in eq. (9) represents the impinging wave; and the second the reflected wave. The time derivative in the neighbourhood of the boundary is now given by:

$$\partial_t \psi = -i\omega\psi = -i\omega\frac{\exp -i\omega t}{4\pi}\left[\frac{\exp ikr}{r} + R\frac{\exp ikr'}{r'}\right] \tag{10}$$

and the space derivatives by:

$$\begin{aligned}
\partial_x\psi &= i\tfrac{\exp -i\omega t}{4\pi}\left[k_x\tfrac{\exp ikr}{r}\left(1+\tfrac{i}{kr}\right)+Rk'_x\tfrac{\exp ikr'}{r'}\left(1+\tfrac{i}{kr'}\right)\right]\\
\partial_y\psi &= i\tfrac{\exp -i\omega t}{4\pi}\left[k_y\tfrac{\exp ikr}{r}\left(1+\tfrac{i}{kr}\right)+Rk'_y\tfrac{\exp ikr'}{r'}\left(1+\tfrac{i}{kr'}\right)\right]\\
\partial_z\psi &= i\tfrac{\exp -i\omega t}{4\pi}\left[k_z\tfrac{\exp ikr}{r}\left(1+\tfrac{i}{kr}\right)+Rk'_z\tfrac{\exp ikr'}{r'}\left(1+\tfrac{i}{kr'}\right)\right]
\end{aligned} \tag{11}$$

where k_x, k_y and k_z are the components of the incident wave number k along the three coordinates, and k'_x, k'_y, and k'_z those of the reflected wave number k'. At the boundary, the distance to the real and imaginary sources are equal, therefore $r = r'$; and $k_x = k'_x$, $k_y = k'_y$, but $k'_z = -k_z$. The partial derivatives further reduce to:

$$\begin{aligned}
\partial_t\psi &= -i\omega\tfrac{\exp -i(\omega t-kr)}{4\pi r}(1+R)\\
\partial_x\psi &= ik_x\tfrac{\exp -i(\omega t-kr)}{4\pi r}(1+R)\left(1+\tfrac{i}{kr}\right) = -\tfrac{k_x}{\omega}\left(1+\tfrac{i}{kr}\right)\partial_t\psi\\
\partial_y\psi &= ik_y\tfrac{\exp -i(\omega t-kr)}{4\pi r}(1+R)\left(1+\tfrac{i}{kr}\right) = -\tfrac{k_y}{\omega}\left(1+\tfrac{i}{kr}\right)\partial_t\psi\\
\partial_z\psi &= ik_z\tfrac{\exp -i(\omega t-kr)}{4\pi r}(1-R)\left(1+\tfrac{i}{kr}\right) = -\tfrac{\beta}{c}\partial_t\psi
\end{aligned} \tag{12}$$

As a consequence, on the boundary, the phase angles ϕ_x and ϕ_y between the space derivatives of the velocity potential with respect to x and y and its time derivative are both equal to $\arctan\frac{1}{kr}$. And eqs. (6) reduce to:

$$D_x = D_y = \Re(\beta) + \frac{\Im(\beta)}{kr}$$

In this case, the imaginary part of the admittance contributes to the scattering coefficient, and this contribution is inversely proportional to kr. And according to the last line of eq. (12), the usual relation between the complex reflection coefficient and the admittance is

113 modified into:

$$R = \frac{\cos\theta\left(1+\frac{i}{kr}\right)-\beta}{\cos\theta\left(1+\frac{i}{kr}\right)+\beta} = \frac{\left[\cos^2\theta\left(1+\frac{1}{k^2r^2}\right)-|\beta|^2\right]-2i\cos\theta\left[\Im\beta+\frac{\Re\beta}{kr}\right]}{\cos^2\theta\left(1+\frac{1}{k^2r^2}\right)+2\cos\theta\left(\Re\beta+\frac{\Im\beta}{kr}\right)+|\beta|^2}$$

114 Note that this expression is equivalent to introducing a complex angle of incidence θ.

115 C. Curved boundary

116 In the case of a curved boundary, the real and virtual sources are not located at the
117 same distance from the boundary (Fig. 4). As a consequence, eqs. (10) and (11) for the
118 partial time and spaces derivative of the velocity potential are still valid in the vicinity
119 of the boundary, provided that x, y and z are now considered as local coordinates at the
120 boundary, the two first ones being parallel to the boundary and the z one perpendicular
121 to it. However, they do not simplify into eq. (12) at the boundary, even though $k_x = k'_x$,
122 $k_y = k'_y$, and $k'_z = -k_z$, because $r' \neq r$.

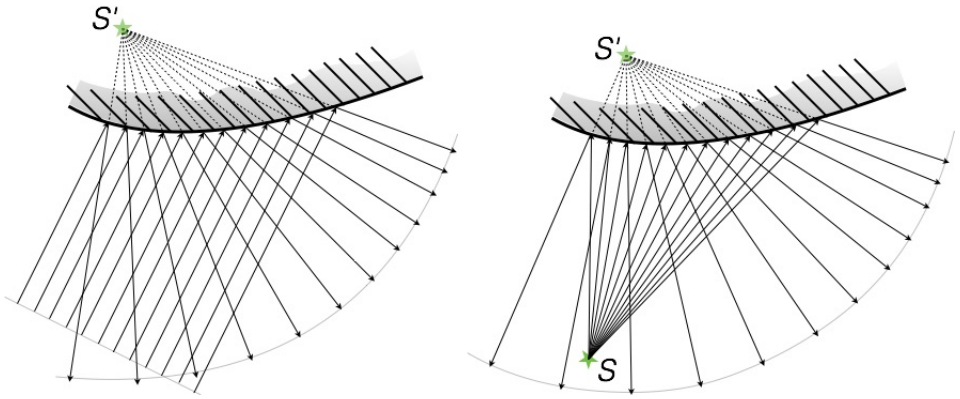

FIG. 4. Reflection on curved boundary. Left: plane wave impinging; right: source at finite distance. S is real source, and S' virtual image source.

On the boundary, we now obtain from eqs. (10) and (11):

$$\partial_x\psi = -\frac{k_x}{\omega}\left(1 + i\frac{\frac{\exp ikr}{kr^2}+R\frac{\exp ikr'}{kr'^2}}{\frac{\exp ikr}{r}+R\frac{\exp ikr'}{r'}}\right)\partial_t\psi$$
$$\partial_y\psi = -\frac{k_y}{\omega}\left(1 + i\frac{\frac{\exp ikr}{kr^2}+R\frac{\exp ikr'}{kr'^2}}{\frac{\exp ikr}{r}+R\frac{\exp ikr'}{r'}}\right)\partial_t\psi$$
$$\partial_z\psi = -\frac{k_z}{\omega}\left(\frac{\left[\frac{\exp ikr}{r}-R\frac{\exp ikr'}{r'}\right]+i\left[\frac{\exp ikr}{kr^2}-R\frac{\exp ikr'}{kr'^2}\right]}{\frac{\exp ikr}{r}+R\frac{\exp ikr'}{r'}}\right)\partial_t\psi = -\frac{\beta}{c}\partial_t\psi$$

where

$$\frac{\left[\frac{\exp ikr}{kr^2}+R\frac{\exp ikr'}{kr'^2}\right]}{\left[\frac{\exp ikr}{r}+R\frac{\exp ikr'}{r'}\right]} = \frac{\left[\frac{1}{kr^2}+\frac{R'}{kr'^2}\right]}{\left[\frac{1}{r}+\frac{R'}{r'}\right]} = \frac{1}{k}\frac{\frac{1}{r^3}+\left(\frac{1}{r}+\frac{1}{r'}\right)\frac{\Re(R')}{rr'}+\frac{|R'|^2}{r'^3}-i\left(\frac{1}{r}-\frac{1}{r'}\right)\frac{\Im(R')}{rr'}}{\frac{1}{r^2}+\frac{2\Re(R')}{rr'}+\frac{|R'|^2}{r'^2}}$$

with

$$\begin{aligned}R' = R\exp ik(r'-r) =& \frac{r'\left[\cos\theta\left(1+\frac{i}{kr}\right)-\beta\right]}{r\left[\cos\theta\left(1+\frac{i}{kr'}\right)+\beta\right]}\\ =& \frac{r'\left[\cos^2\theta\left(1+\frac{1}{k^2rr'}\right)+\cos\theta\frac{\Im\beta}{k}\left(\frac{1}{r}-\frac{1}{r'}\right)-|\beta|^2\right]}{r\left[\cos^2\theta\left(1+\frac{1}{k^2r'^2}\right)+2\cos\theta\left(\Re\beta+\frac{\Im\beta}{kr'}\right)+|\beta|^2\right]}\\ &+ i\frac{r'\cos\theta\left[\frac{\cos\theta}{k}\left(\frac{1}{r}-\frac{1}{r'}\right)-2\Im\beta+\frac{\Re\beta}{k}\left(\frac{1}{r}+\frac{1}{r'}\right)\right]}{r\left[\cos^2\theta\left(1+\frac{1}{k^2r'^2}\right)+2\cos\theta\left(\Re\beta+\frac{\Im\beta}{kr'}\right)+|\beta|^2\right]}\end{aligned} \tag{13}$$

We then obtain:

$$\tan\phi_x = \tan\phi_y = \frac{1}{k}\frac{\frac{1}{r^3}+\left(\frac{1}{r}+\frac{1}{r'}\right)\frac{\Re(R')}{rr'}+\frac{|R'|^2}{r'^3}}{\frac{1}{r^2}+\frac{2\Re(R')}{rr'}+\frac{|R'|^2}{r'^2}+\left(\frac{1}{r}-\frac{1}{r'}\right)\frac{\Im(R')}{krr'}} \tag{14}$$

As a consequence, the phase angles ϕ_x and ϕ_y between the space derivatives of the velocity potential with respect to x and y and its time derivative are position dependent - and depend on the local angle of incidence θ - through the modified reflection coefficient R'. No simple equation subsists for eqs. (6) to reduce to.

Note that, in the case of a plane wave incident on a curved boundary (left pane of Fig. 4), recalculating eqs. (13) and (14) gives the simpler formulas:

$$R' = \frac{r'\left[\cos\theta - \beta\right]}{\cos\theta\left(1+\frac{i}{kr'}\right)+\beta} = r'\frac{\left[\cos^2\theta - \cos\theta\frac{\Im\beta}{kr'} - |\beta|^2\right] - i\cos\theta\left[\frac{\cos\theta}{kr'} + 2\Im\beta - \frac{\Re\beta}{kr'}\right]}{\cos^2\theta\left(1+\frac{1}{k^2r'^2}\right) + 2\cos\theta\left(\Re\beta + \frac{\Im\beta}{kr'}\right) + |\beta|^2}$$

$$\tan\phi_x = \tan\phi_y = \frac{1}{kr'^2}\frac{\Re(R') + \frac{|R'|^2}{r'}}{1 + \frac{2\Re(R')}{r'} + \frac{|R'|^2}{r'^2} - \frac{\Im(R')}{kr'^2}}$$

VI. DISCUSSION

A. Absorption coefficient

The form for the absorption coefficient given by eq. (5) does not reduce to the form given by Morse and Ingard (Added: (Morse and Ingard, 1968, p. 580)) and introduced in acoustics by Paris (Paris, 1927). However, but for a constant multiplicative factor, it is similar to an expression given by Bosquet (Bosquet, 1967). As Bosquet further explains, the form taken by the absorption coefficient strongly depends on the weighting function, that is, the statistics one chooses for computing the mean absorption coefficient. In the present case, the obvious choice is the so-called star-type statistics introduced by London (London, 1950), that is, taking the mean value of the equation $E_{tz} = \alpha E_{tt}$:

$$\int_0^{\frac{\pi}{2}} E_{tz}\sin\theta d\theta = \alpha^* \int_0^{\frac{\pi}{2}} E_{tt}\sin\theta d\theta \tag{15}$$

Compared to the more usual bar-type statistics (Bosquet, 1967; London, 1950), the star-type statistics does not include the factor $\cos\theta$; but there is no need to introduce this factor as E_{tz} already contains it, since it is the normal flux into the wall. Therefore is the star-type statistics the obvious choice. Assuming as usual an isotropic distribution of wave directions,

the term $|\partial_t \psi|^2$ is then constant for all wave directions in the first line of eq. (3) and in eq. (4). The left hand side of eq. (15) simply reduces to the mean value of $\sin\theta$; and the right hand side also includes the mean value of $\sin^3\theta$. Therefore, one obtains:

$$\alpha^* = \frac{2\,\Re(\beta)}{1+\frac{2}{3}+|\beta|^2} \tag{16}$$

which is the value of $\alpha(\theta)$ taken for $\theta = 55^o$, an angle that has repeatedly appeared since the 1950s as the incidence angle that represents the mean absorption (Bosquet, 1967; Guignouard, 1991; Vogel, 1956). Indeed, $\sin^2 55^o = 0.67 \approx \frac{2}{3}$.

Simple calculation shows that the absorption coefficients given by eq. (5) and (16) take values between 0 and a maximum reached when $\Re(\beta) = \sqrt{1+\sin^2\theta+\Im^2(\beta)}$ and $\Re(\beta) = \sqrt{1+\frac{2}{3}+\Im^2(\beta)}$ respectively. This maximum is respectively equal to $\frac{1}{\sqrt{1+\sin^2\theta+\Im^2(\beta)}}$ and $\frac{1}{\sqrt{1+\frac{2}{3}+\Im^2(\beta)}}$, that is, reaches its absolute maximum for $\Im(\beta) = 0$ with value $\frac{1}{\sqrt{1+\sin^2\theta}}$ and $\frac{1}{\sqrt{1+\frac{2}{3}}} \approx 0.775$ respectively. Both absolute maxima are therefore smaller than 1, except at normal incidence ($\theta = 0$) for the first one.

Last but not least, integrating eq. (16) on octave or third octave energy bands leads to the usual definition of band related absorption coefficients.

B. Scattering coefficients

The scattering coefficients given by eq. (6) are independent of the incidence angle θ, except through the reflection coefficient in the expression of $\tan\phi_x$ and $\tan\phi_y$ for curved boundaries. However, the real part of the wall admittance contributes to the scattering

coefficients. In other words, absorption on the wall induces scattering. This is a novel result.

Also novel is the observation that scattering coefficients are not bounded: they can take any value between $-\infty$ and $+\infty$, as is easily seen from eq. (6).

Traditionally, scattering is considered as the result of two mechanisms (Embrechts, 2002): finite dimensions of reflecting surfaces; and roughness of the reflecting surfaces. There is no doubt from Sect. V C that the second term of eq. (6) corresponds to scattering by surface roughness, since it is driven by the finite distance from the surface to the image source. However, this term subsists for sources located at finite distances from a flat reflecting surface (see Sect. V B), as long as its admittance admits an imaginary part. But roughness is usually associated with locally varying imaginary parts of the admittance, as can be easily demonstrated with Schroeder diffusers, where the depths of the wells drive this imaginary part. In the present case, no locally varying admittance is necessary to induce scattering.

We therefore suspect that the mechanism described in Sect. V does not correspond to traditional scattering, but to a different effect. Indeed, in the work of Dujourdy *et al.* (Dujourdy *et al.*, 2017, 2019) and Meacham *et al.* (Meacham *et al.*, 2019), the scattering coefficient induces a decrease of steady-state energy with distance. Although scattering does induce a decrease of steady-state energy with distance by redirecting part of it toward the source, no redirection is here at stake, just a reduction of the acoustical intensity by friction on the walls. In other words, total energy and acoustical intensity can be considered as two coupled systems that each follow its own conservation equation with some exchange

between the two systems. As is well known from such coupled systems, the less damped system drives the energy decay with time, which precisely is what is obtained in Fig. 1.

As a consequence, the scattering coefficient D is ill-named. A better designation would be *intensity-friction* coefficient, or simply *friction* coefficient. For the time being, we stick to usage and keep the designation "scattering coefficient".

Note that, as for the absorption coefficient, integrating eq. (6) on octave or third octave energy bands leads to band related scattering - or friction - coefficients.

C. Admittance, impedance, and acoustic resistance

From the expression of the absorption and scattering coefficients (eqs. 5 and 6), it becomes possible to express the (Replaced: ~~reduced~~ replaced with: specific acoustic) admittance in the case of flat walls, which is the case of Fig. 1. From this expression, the (Replaced: ~~reduced~~ replaced with: specific acoustic) impedance and the acoustic resistance of the wall can also be computed.

Table I presents the value of the octave-band absorption and scattering coefficients of the hallway of Fig. 1, derived from the figure itself by taking the centre of the vertical green patches. (Added: There is no green patch in Fig. 1 for the 125 Hz octave band, but the two stripes are tangent to each other at the point used in Table I.) Note that, according to eq. (6), the real part of the (Replaced: ~~reduced~~ replaced with: specific acoustic) admittance is equal to the scattering coefficient (plane walls). The imaginary part is obtained from eq. (5) which gives valid values for all octave bands. Two possibilities exist here: either considering a diffuse sound field, and use the average absorption coefficient of eq. (16); or considering

that the sound field remains parallel to the walls, and use eq. (5) with $\sin\theta = 0$. The latter case gave more consistent results.

The (Replaced: ~~reduced~~ replaced with: specific acoustic) impedance is then computed as the inverse of the (Replaced: ~~reduced~~ replaced with: specific acoustic) admittance, and multiplying its real part by the characteristic impedance (Added: of air) $\rho_0 c = 410$ Ns/m^3 approximates the acoustic resistance of the wall - also in Ns/m^3. No attempt has been made to compare the obtained values to typical walls, given that they are made of particle boards and gyps boards, with a hard plastic floor. Indeed, quick evaluation of the resonances of the walls by knocking on them revealed a complex structure with many resonances spread over all the octave bands of interest, rendering inconsistent the parsing of the measured impedance into resonances.

VII. CONCLUSION

Starting with the precedent papers of Dujourdy *et al.* (Dujourdy *et al.*, 2017, 2019) that have shown that integrating the stress-energy tensor in a disproportionate enclosure and taking into account the boundary conditions leads to "loss terms" that correspond to absorption and scattering, we expressed the elements of the stress-energy tensor with the help of the wall admittance relation between normal derivative and time derivative of the velocity potential on the wall.

As expected, the absorption coefficients are proportional to the real part of the wall admittance. However, they also depend on the angle of incidence of the wave, leading to an expression of the absorption coefficient eq. (16) which has been signaled in the literature,

TABLE I. Admittance, impedance and acoustic resistance of the walls of the hallway of Fig. 1.

octave band	63Hz	125Hz	250Hz	500Hz	1kHz	2kHz	4kHz	8kHz
absorption coeff.	0.025	0.115	0.1	0.095	0.09	0.12	0.14	0.13
scattering coeff.	0.6	0.125	0.335	0.355	0.22	0.135	0.145	0.23
$\Re(\beta)$	0.6	0.125	0.335	0.355	0.22	0.135	0.145	0.23
$\Im(\beta)$	6.83	1.08	2.036	2.52	1.96	1.11	1.02	1.58
$\Re(\zeta)$	0.013	0.106	0.059	0.055	0.057	0.108	0.135	0.091
$\Im(\zeta)$	-0.15	-0.92	-0.41	-0.39	-0.50	-0.89	-0.96	-0.62
resistance (Ns/m^3)	5.23	43.7	24.1	22.5	23.2	44.3	55.5	37.1

for example by Bosquet (Bosquet, 1967), yet is not very usual; and to scattering coefficients additively involving the real and imaginary parts of the wall admittance, as seen in eq. (6), proving the absorptive nature of the scattering coefficient in the stress-energy tensor formalism.

In the case of plane boundaries, calculations can be extended to evaluate the mean impedance of the walls. An example is given for a long hallway.

ACKNOWLEDGMENTS

AUTHOR DECLARATIONS

Conflict of Interest

The authors have no conflicts to disclose.

Data Availability

Data sharing not applicable no new data generated.

Bosquet, J. (**1967**). "La théorie synthétique de la réverbération," in *Bulletin du Laboratoire d'Acoustique de l'Université de Liège 11*, pp. 51–67.

Dujourdy, H., Pialot, B., Toulemonde, T., and Polack, J.-D. (**2017**). "Energetic wave equation for modelling diffuse sound field - Applications to corridors," Acta Acust united Ac **103**(3), 480–491.

Dujourdy, H., Pialot, B., Toulemonde, T., and Polack, J.-D. (**2019**). "Energetic wave equation for modelling diffuse sound field - Applications to open offices," Wave Motion **87**, 193–212.

Embrechts, J.-J. (**2002**). "Modlisation des réflexions diffuses en acoustique des salles : état de la question," in *6ème Congrès Franais d'Acoustique*, pp. 666–669.

Guignouard, P. (**1991**). "L'absorption acoustique des matériaux poreux - prédictions et mesures," Ph.D. thesis, Université du Maine.

London, A. (**1950**). "The determination of reverberant sound absorption coefficients from acoustic impedance measurements," J. Acoust. Soc. Am. **22**(2), 263–269.

Mann, J., Tichy, J., and Romano, A. (**1987**). "Instantaneous and time-averaged energy transfer in acoustic fields," J. Acoust. Soc. Am. **82**(1), 17–30.

Meacham, A., Badeau, R., and Polack, J. D. (**2019**). "Lower bound on frequency validity of energy-stress tensor based diffuse sound field model," in *23rd International Congress on Acoustics*.

Morse, P. M., and Feshbach, H. (**1956**). *Mathematical Methods of Theoretical Physics* (Mc Graw-Hill Book Company).

Morse, P. M., and Ingard, K. U. (**1968**). *Theoretical Acoustics* (Mc Graw-Hill Book Company).

Ollendorff, F. (**1969**). "Statistical room acoustics as a problem of diffusion, a proposal," Acustica **21**, 236–245.

Paris, E. T. (**1927**). "On the reflexion of sound from a porous surface," Proc. R. Soc. Lond. A **115**, 407–419.

Picaut, J., Simon, L., and Polack, J. D. (**1997**). "A mathematical model of diffuse sound field based on a diffusion equation," Acta Acust united Ac **83**(4), 614–621, http://www.ingentaconnect.com/content/dav/aaua/1997/00000083/00000004/art00006.

Polack, J. (**2023**). "Energy relationships in enclosures," in *forum acusticum 2023*.

Stanzial, D., Bonsi, D., and Schiffrer, G. (**2002**). "Four dimensional treatment of linear acoustic fields and radiation pressure," Acta Acust. united Ac. **89**(2), 213–224, https://www.ingentaconnect.com/content/dav/aaua/2003/00000089/00000002/art00002.

Stanzial, D., and Graffigna, C. E. (**2017**). "On the general connection between wave impedance and complex sound intensity," Proc. Mtgs. Acoust. **30**(1), 055013, https://doi.org/10.1121/2.0000797.

Stanzial, D., and Schiffrer, G. (**2010**). "On the connection between energy velocity, reverberation time and angular momentum," J. Sound Vib. **329**(7), 931–943, https://doi.org/10.1016/j.jsv.2009.10.011.

Vogel, T. (**1956**). "Sur les propriétés acoustiques des matériaux," L'Onde Electrique **36**, 428–434.

List of Changes

Added: The stress-energy tensor formalism was initially introduced by Morse and collaborators (Morse and Feshbach, 1956; Morse and Ingard, 1968) in order to describe energy conservation in linear acoustics. Many years later, Stanzial and collaborators applied the conservation of the stress-energy tensor to room acoustics (Stanzial *et al.*, 2002), focusing on the expression of the radiation pressure. In a subsequent paper (Stanzial and Schiffrer, 2010), they introduced the energy velocity as ratio of the sound intensity to the total acoustic energy, and derived from the conservation of the stress-energy tensor an expression for the local inital reverberation time at the onset of energy decay. Some related ideas, linking wave impedance to the complex sound intensity, are also found

in (Mann *et al.*, 1987; Stanzial and Graffigna, 2017). Mann *et al.* focused on energy transfer and analysed in terms of energy flux and power what happens in the vicinity of intensity vortex that are created by specific configurations of sources. Stanzial and Graffigna went one step further in the definition and measurement of complex intensity. However, both papers are outside the scope of the present analysis that focuses on the active stress-energy tensor - see (Polack, 2023) for an extension to the *complex* stress-energy tensor and its conservation, together with preliminary measurement results., on page 2, line 12.

Replaced: ~~The stress-energy tensor formalism~~ replaced with: A somewhat different perspective, on page 2, line 27.

Added: in order, on page 2, line 28.

Added: steady-state, on page 4, line 50.

Replaced: ~~reduced~~ replaced with: specific acoustic, on page 5, line 67.

Added: (Morse and Ingard, 1968, p. 580), on page 5, line 67.

Added: that is, the wall impedance normalized by the characteristic impedance $\rho_0 c$ of air,, on page 5, line 67.

Added: is, on page 6, line 67.

Replaced: ~~reduced~~ replaced with: specific acoustic, on page 6, line 67.

Added: Note that E_{xz} and E_{yz} correspond to the parallel components of the radiation pressure exerted on the "ceiling" and the "floor" (Stanzial *et al.*, 2002)., on page 7, line 69.

Added: (Morse and Ingard, 1968, p. 580), on page 15, line 130.

Replaced: ~~reduced~~ replaced with: specific acoustic, on page 18, line 189.

Replaced: ~~reduced~~ replaced with: specific acoustic, on page 18, line 190.

Added: There is no green patch in Fig. 1 for the 125 Hz octave band, but the two stripes are tangent to each other at the point used in Table I., on page 18, line 195.

Replaced: ~~reduced~~ replaced with: specific acoustic, on page 18, line 197.

Replaced: ~~reduced~~ replaced with: specific acoustic, on page 19, line 203.

Replaced: ~~reduced~~ replaced with: specific acoustic, on page 19, line 204.

Added: of air, on page 19, line 205.